

Type I interferon restricts mRNA vaccine efficacy through suppression of antigen uptake in cDCs

Received: 11 July 2025

Accepted: 18 December 2025

Cite this article as: Lobb, T.A., Dickson, A., Guo, W. *et al.* Type I interferon restricts mRNA vaccine efficacy through suppression of antigen uptake in cDCs. *npj Vaccines* (2025). <https://doi.org/10.1038/s41541-025-01362-z>

Tyson A. Lobb, Alexandria Dickson, Wenzheng Guo, Smrithi Beeram, Javier A. Carrero, Yago Dalben, Richard J. DiPaolo, Elise Alspach, Longping V. Tse & Stephen T. Ferris

We are providing an unedited version of this manuscript to give early access to its findings. Before final publication, the manuscript will undergo further editing. Please note there may be errors present which affect the content, and all legal disclaimers apply.

If this paper is publishing under a Transparent Peer Review model then Peer Review reports will publish with the final article.

Type 1 Interferon Restricts mRNA vaccine Efficacy Through Suppression of Antigen Uptake in cDCs

Tyson A. Lobb¹, Alexandria Dickson², Wenzheng Guo¹, Smrithi Beeram¹, Javier A. Carrero¹, Yago Dalben¹, Richard J. DiPaolo¹, Elise Alspach¹, Longping V. Tse¹, and Stephen T. Ferris¹⁺

¹Department of Molecular Microbiology and Immunology, Saint Louis University School of Medicine, St. Louis, MO.

²Department of Immunology and Microbiology, University of Colorado Anschutz Medical Campus, Aurora, CO.

+ Corresponding author

Corresponding author information:

Stephen T. Ferris
1100 S Grand Blvd
Rm 617
St. Louis MO 63104
314-977-8788
stephen.ferris@health.slu.edu

COI disclosure statement

The authors declare no conflicts of interest.

Abstract

Type I interferons (IFN) are key mediators of innate immune activation, promoting upregulation of costimulatory molecules and Major Histocompatibility Complex (MHC) I/II on antigen presenting cells (APCs). However, IFN also suppress endogenous translation to restrict viral replication. Critically, IFN-stimulated APCs lose the capacity to acquire new antigens, making the timing of IFN signaling a crucial determinant of vaccine efficacy. Here, we show that both DC-specific loss of IFN α/β receptor (IFN α R) and transient blockade of IFN α R before vaccination enhances vaccine uptake and expression within DCs, improves CD8 $^{+}$ T cell priming, and leads to superior tumor control. We also demonstrate that IFN signaling before vaccination, triggered by prior infection or administration of a different vaccine, impairs dendritic cell uptake of mRNA-LNP vaccines and reduces the magnitude of vaccine-specific CD8 $^{+}$ T cell responses. These findings highlight the dual-edged nature of IFN signaling and offer a potential strategy for enhancing vaccine-induced immunity.

Introduction

mRNA-based vaccines have revolutionized vaccinology. Beyond its major impact in aiding to resolve the COVID-19 pandemic, the potential of mRNA-based therapeutics is vast, with applications extending from viruses like influenza¹ and human immunodeficiency virus^{2,3} to cancer^{4–6}. Notably, mRNA-based neoantigen therapies for hard-to-treat pancreatic cancer are already currently in clinical trials⁷. Therefore, it is critical to understand the underlying immune mechanisms governing their response and how to augment the efficacy of mRNA-lipid nanoparticle (mRNA-LNP) vaccines. It is well established that mRNA-LNPs induce type 1 interferons (IFN) (e.g., IFN- α , IFN- β)

upon immunization^{8–11}. IFN plays a critical role in antiviral immune responses by limiting viral spread and activating innate immunity to elicit long-lasting adaptive immunity¹². IFN signaling has been shown to be required for CD8⁺ T cells to develop their cytotoxic capacity¹³ and plays a crucial role in augmenting antigen-presenting cell (APC) activation and the priming of adaptive immune responses^{14,15}. IFN signaling in APCs at the time of antigen acquisition has been shown to significantly enhance the subsequent adaptive immune response through upregulation of costimulatory molecules and promotion of inflammatory cytokine production. Thus, IFN has canonically been thought to augment or induce immune responses. However, multiple studies have shown that chronic IFN signaling is detrimental to the overall immune response, leading to immune suppression^{16–20}. It has also been shown that once a conventional dendritic cell (cDC) or APC is activated and matures, it can no longer acquire new material for presentation to the adaptive immune system^{21,22}. Similarly, previous research showed that migratory, or mature, DCs are unable to acquire new cell-associated material for presentation to CD8⁺ T cells²³. This suggests that the *timing* of APC activation may determine whether IFN acts as a stimulatory or inhibitory factor in APC-mediated antigen processing and presentation: a fully mature or activated APC is incapable of processing and presenting new antigens. Recent studies suggest that IFN signaling can also suppress adaptive immune responses during viral infections. Notably, transient blockade of IFN signaling using the IFN α R blocking antibody MAR1-5A3²⁴ (α IFN α R) has been shown to enhance virus-specific immune responses²⁵. Similarly, a recent publication found that transient IFN α R blockade enhanced virus-specific immune responses in the context of an arthritogenic alphavirus²⁶. Still, the underlying mechanisms remain unclear.

In the context of vaccination, transient IFN α R inhibition, as well as the use of IFN α R-deficient mice or tissue-specific IFN α R deletion, have yielded variable outcomes. A recent article demonstrated that blocking IFN signaling reduced overall CD8 $^{+}$ and CD4 $^{+}$ T cell responses following mRNA-LNP vaccination¹¹. In contrast, a separate study found that transient IFN α R blockade during LCMV infection and vaccination enhanced the generation of virus- or vaccine-specific stem cell-like memory CD8 $^{+}$ T cells²⁷. Thus, the role of IFN in vaccines, including mRNA-LNP-based vaccines, remains unclear, with evidence supporting both inhibitory and augmentative effects.

In this study, we aimed to elucidate the role of IFN signaling during mRNA-LNP-based vaccination by utilizing transient IFN α R blockade and mice with DC-specific loss of IFN α R. Given the inhibitory impacts of inflammatory cytokine signaling on DC antigen acquisition, we hypothesized that early IFN signaling within DCs impairs their ability to acquire and translate the new antigenic mRNA, thereby limiting antigen presentation and ultimately leading to a diminished adaptive immune response. Understanding this dynamic may provide insight into the timing and regulation of IFN signaling in optimizing vaccine efficacy.

Results

mRNA-LNP vaccine induced IFN reduces vaccine-specific mRNA expression by DCs *in vitro*

To assay if IFN signaling inhibited acquisition of mRNA-LNP, we generated bone marrow-derived DCs (BMDCs) using a novel culture method with stem cell factor (SCF) and FMS-like tyrosine kinase 3 ligand (Flt3L)²⁸. This protocol enhances DC output and produces subsets of conventional DCs that closely resemble their *in vivo*-derived counterparts (Supplementary Fig. 1). To assess mRNA-LNP vaccine uptake, we incubated BMDCs with eGFP mRNA-LNP vaccines and measured eGFP expression by flow cytometry. 16-hour pretreatment of BMDCs with IFN α completely abrogated eGFP expression, resulting in no increase of eGFP expression above PBS incubated controls (Fig. 1A). This suggests that premature activation of BMDCs through IFN α R signaling inhibited mRNA-LNP acquisition and expression. Given the rapid nature of IFN signaling²⁹, we hypothesized that once a cell senses mRNA-LNP, it produces IFN, which in turn suppresses mRNA-LNP uptake by surrounding DCs. To test this, we blocked IFN α R signaling at the time of mRNA-LNP administration using anti-IFN α R blocking antibody MAR1-5A3. Blocking IFN signaling during mRNA-LNP administration increased the proportion of DCs acquiring and expressing eGFP (Fig. 1A). When assessing the DC activation marker CD40, IFN α pretreatment and mRNA-LNP alone uniformly activated all DCs, whereas IFN α R blockade significantly reduced CD40 upregulation (Fig. 1B). These findings suggest that inhibiting premature IFN-mediated DC activation enhances mRNA-LNP uptake and expression by DCs *in vitro*.

Inhibition of IFN α R signaling enhances dendritic cell acquisition of mRNA-LNPs and improves vaccine-specific CD8 $^{+}$ T cell responses.

To determine whether blocking IFN α R signaling enhances DC acquisition of mRNA-LNPs *in vivo*, we first confirmed that IFN is produced following immunization with our mRNA-LNP vaccine. IFN α 2 and 4 were found in the serum of immunized WT C57BL/6J mice at 8 hours and was absent by 24 hours post vaccination, in agreement with previous findings showing IFN production is early and transient post mRNA-LNP vaccination⁶ (Fig. 2A). Previous studies have shown that administering 100ug of IFN α R blocking antibody MAR1-5A3 reduces surface expression of IFN α R1 for five days, with receptor expression returning by day six²⁵. We verified these results; however, we saw that MAR1-5A3 antibody used at 250ug reduced IFN α R1 surface expression for at least 9 days post injection with expression not returning to control WT C57BL/6J levels over the experimental time course (Fig. 2B). Next, we asked whether blocking the IFN α R receptor before immunization with an eGFP mRNA-LNP vaccine would increase DC mRNA-LNP acquisition and translation. To test this, we blocked IFN α R one day before immunizing mice with an eGFP mRNA-LNP vaccine. Splenic cDCs (Supplementary Fig. 2A) were isolated 24 hours post-immunization and analyzed for eGFP expression by flow cytometry. IFN α R inhibition significantly increased the number of splenic DCs expressing eGFP compared to unblocked controls (Fig. 2C). In terms of DC activation, both eGFP and OVA mRNA-LNP vaccines induced upregulation of the activation markers CD40 and CD86 on splenic DCs; however, IFN α R blockade substantially reduced CD40 and CD86 expression compared to unblocked, immunized mice. Despite this reduction, activation levels in IFN α R-blocked, eGFP-vaccinated mice remained higher than in PBS-immunized controls (Fig. 2D). In addition, DCs that had acquired eGFP mRNA-LNP were activated, albeit less than unblocked controls (Supplementary

Fig. 3A). Moreover, blocking IFN α R signaling during immunization did not alter overall DC numbers (Supplementary Fig. 3B). Thus, inhibition of IFN α R signaling leads to an increase in DC mediated mRNA-LNP acquisition and expression. With this in mind, we next asked whether blocking the IFN α R receptor before immunization with the OVA mRNA-LNP vaccine would increase vaccine-specific CD8 $^{+}$ T cells. Blocking IFN α R prior to immunization significantly increased vaccine-specific CD8 $^{+}$ T cells (Supplementary Fig. 2B, 3C, and Fig. 2E). In addition, vaccine-specific CD8 $^{+}$ T cells expressed higher surface levels of PD-1 (Fig. 2F), potentially pointing to increased T cell receptor signaling due to increased antigen presentation^{30,31}. To ensure that blocking IFN α R increased mRNA-LNP acquisition and not merely mRNA translation, we immunized mice with mRNA-LNP incorporated with the fluorescent lipid 1,1'-dioctadecyl-3,3,3',3'-tetramethylindodicarbocyanine (DiD) which incorporates into the endosomal membrane once acquired by cells³². IFN α R inhibition 24 hours prior to immunization significantly increased the number of splenic DCs that acquired and expressed the fluorescent LNP compared to unblocked controls indicating an increase in mRNA-LNP acquisition by DCs. (Fig. 2G). These findings support our hypothesis that inhibiting IFN α R signaling prevents bystander DC activation, allowing for enhanced mRNA-LNP uptake and subsequent adaptive immune priming.

DC specific loss of IFN α R increases vaccine-specific CD8 $^{+}$ T cell responses

To further test the notion that IFN signaling inhibits mRNA-LNP vaccine acquisition and antigen presentation specifically in DCs we assayed mRNA-LNP vaccine responses in mice that lack DC-specific expression of IFN α R. We utilized the CD11c cre (*Itgax*^{cre})³³

mice which have dendritic cell-specific expression of cre recombinase crossed to mice which contain LoxP sites flanking exon 3 of *Ifnar*³⁴ (*Ifnar*^{f/f}) to test DC-specific deletion of IFN α R. We immunized *Itgax*^{cre} *Ifnar*^{f/f} (*Ifnar*^{cKO}) and *Ifnar*^{f/f} (*Ifnar*^{WT}) mice with mRNA-LNP vaccines and assayed for eGFP expression at 24 hours. DCs from *Ifnar*^{cKO} mice had a significantly higher proportion of splenic DCs expressing eGFP compared to *Ifnar*^{WT} controls (Fig. 3A). Similarly, *Ifnar*^{cKO} DCs were significantly less activated as evidenced by surface expression of CD40 and CD86 when compared to *Ifnar*^{WT} controls (Fig. 3B). Similar to blocking IFN α R signaling during immunization, DC-specific deletion of *Ifnar* did not alter overall DC numbers after immunization (Supplementary Fig. 4A). These findings support the notion that IFN α R signaling within DCs limits mRNA-LNP uptake and expression. Next, we assayed if DC-specific loss of IFN α R could enhance CD8 $^{+}$ T cell responses to mRNA-LNPs. We immunized *Ifnar*^{cKO} and *Ifnar*^{WT} mice with OVA mRNA-LNP vaccines and measured vaccine-specific CD8 $^{+}$ T cell responses 7 days later. *Ifnar*^{cKO} mice displayed a significant increase in vaccine-specific CD8 $^{+}$ specific T cells as compared to *Ifnar*^{WT} control mice (Supplementary Fig. 4B, and Fig. 3C). In addition, *Ifnar*^{cKO} vaccine-specific CD8 $^{+}$ T cells displayed an increased surface expression of PD-1 as compared to *Ifnar*^{WT} controls (Fig. 3D). Again, to ascertain if this effect was due to an increased ability for DCs to acquire the mRNA-LNP, we immunized *Itgax*^{cre} *Ifnar*^{f/f} (*Ifnar*^{cKO}) and *Ifnar*^{f/f} (*Ifnar*^{WT}) mice with mRNA-LNP incorporated with a fluorescently labelled LNP, as in Figure 2G. Twenty four hours after immunization with fluorescently labeled mRNA-LNP, splenic DCs from *Ifnar*^{cKO} mice displayed a significantly higher expression of the fluorescent LNP compared to *Ifnar*^{WT} control DCs indicating an increased ability to acquire the mRNA-LNP (Fig. 3E). These findings

resembled those observed when IFN α R was blocked systemically by the MAR1-5A3 antibody (Fig. 2C-G). Our results show that loss of IFN α R signaling specifically in DCs is sufficient to enhance mRNA-LNP vaccine immune responses through increased mRNA-LNP uptake and expression.

Inducing IFN before mRNA-LNP vaccination reduces vaccine efficacy

Previous studies have shown that DCs cease acquiring exogenous antigens after activation²¹. Based on this, we hypothesized that inducing IFN prior to administering our OVA mRNA-LNP vaccine would suppress the OVA-specific immune response. To test this hypothesis, we immunized mice with PBS or with eGFP mRNA-LNP to induce transient IFN production 24 hours before administering the OVA mRNA-LNP vaccine (Fig. 4A). Immunization with eGFP mRNA-LNP 24 hours before OVA mRNA-LNP immunization significantly reduced OVA-specific CD8 $^{+}$ T cell responses (Fig. 4B). However, when we blocked IFN α R signaling prior to administering both mRNA-LNP vaccines, generation of vaccine OVA-specific CD8 $^{+}$ T cells was restored (Fig. 4B). While surface level expression of PD-1 was not significantly different on vaccine-specific CD8 $^{+}$ T cells with or without MAR1-5A3 treatment, there is trend towards higher PD-1 MFI in IFN α R blocked mice (Fig. 4C).

To ascertain if these results were driven by IFN signaling specifically in DCs, we immunized *Ifnar*^{cKO} and *Ifnar*^{WT} mice with the eGFP mRNA-LNP vaccine followed by immunization with our OVA mRNA-LNP vaccine (Fig. 4D). As expected, *Ifnar*^{WT} mice immunized with eGFP mRNA-LNP prior to OVA mRNA-LNP vaccination displayed

significantly reduced OVA-specific CD8⁺ T cell responses compared to *Ifnar*^{WT} mice immunized with OVA mRNA-LNP vaccine alone (Fig 4E). In contrast, no decrease in CD8⁺ T cell response was observed in *Ifnar*^{CKO} mice immunized with eGFP mRNA-LNP followed by OVA mRNA-LNP vaccines (Fig. 4E). Additionally, *Ifnar*^{CKO} mice immunized with both eGFP mRNA-LNP and OVA mRNA-LNP vaccines displayed a significant increase in PD-1 expression on OVA vaccine-specific CD8⁺ T cells compared to those from *Ifnar*^{WT} immunized with both eGFP mRNA-LNP and OVA mRNA-LNP vaccines or OVA mRNA-LNP vaccines alone (Fig. 4F). Thus, immunizing with mRNA-LNP vaccines when systemic IFN is present or recently induced, either due to a prior vaccination or other IFN inducing agent, reduces the effectiveness of the vaccine-specific CD8⁺ T cell response. This effect is likely due to premature DC activation.

Dendritic cells are essential for generating vaccine-specific CD8⁺ T cell responses to mRNA-LNP immunization.

Because we found that IFNaR signaling in DCs alters how mRNA-LNPs are acquired and presented, we next wanted to determine whether DCs are the primary APCs responsible for presenting mRNA-LNP-derived antigens. To test this, we used the *Itgax*-HBEGF/EGFP (CD11c-DTR) mouse model, which allows for an inducible depletion of DCs via expression of the diphtheria toxin receptor (DTR) on CD11c⁺ cells. Upon administration of diphtheria toxin (DTX), CD11c⁺ DCs are selectively ablated through toxin-induced cell death (Fig 5A). We then evaluated whether vaccine-specific CD8⁺ T cells could be generated in the absence of DCs. For this, we administered DTX to CD11c-DTR mice one day prior to immunization with OVA mRNA-LNPs and continued

DTX treatment every other day until day 7, when we assessed CD8⁺ T cell responses. CD11c-DTR mice treated with DTX showed a marked reduction in vaccine-specific CD8⁺ T cells compared to DTX-treated WT mice and vehicle-treated CD11c-DTR mice (Fig. 5B). While we observed a slight increase in PD-1 expression on vaccine-specific DTX treated WT mice, PD-1 levels remained equivalent amongst the experimental groups (Fig. 5C). These results demonstrate that DCs are essential for the mRNA-LNP vaccine response in our model and are critical for eliciting vaccine-specific CD8⁺ T cell responses.

cDC1s are the major DC subset priming the CD8⁺ T cell mRNA-LNP vaccine immune response

We next wanted to determine if a specific subset of cDC was the major antigen presenting cell to create OVA vaccine-specific CD8⁺ cells. To assay this, we used an *Irf8* +32 enhancer knockout mouse (Δ 32) which lack the conventional dendritic cell type 1 (cDC1) subset³⁵ and the *Zeb2* triple enhancer knockout mouse (Δ 1+2+3) which lack the conventional dendritic cell type 2 (cDC2) subset (Fig. 6 A, B)³⁶. We immunized Δ 32 and Δ 1+2+3 mice with OVA mRNA-LNP vaccines and assayed vaccine-specific CD8⁺ T cell responses 7 days later. At 7 days post immunization, Δ 32 mice had an almost complete loss in the ability to produce vaccine-specific CD8⁺ T cells (Fig. 6C). While priming of vaccine-specific CD8⁺ specific T cells was nearly absent in Δ 32 mice, Δ 1+2+3 mice displayed a striking increase in vaccine-specific CD8⁺ T cells compared to WT controls (Fig 6C). We also found that the few vaccine-specific CD8⁺ T cells produced in Δ 32 mice displayed significantly lower surface expression of PD-1 compared to both

vaccine-induced CD8⁺ T cells from WT and $\Delta 1+2+3$ mice (Fig 6D). In summary, our data indicate that the cDC1 subset is largely responsible for driving mRNA-LNP vaccine immune responses.

Virus induced responses reduces mRNA-vaccine efficacy

Because IFN inhibits mRNA-LNP vaccine efficacy, we asked if IFN induced during viral infection could inhibit subsequent mRNA-LNP vaccine efficacy. To test this, we used a non-lethal viral infection model of mouse adapted Dengue virus (D220). Although D220 infection in C57BL/6J mice does not lead to weight loss, mice that are infected with this virus can still induce inflammatory cytokines including type I and II IFN as well as TNF- α ³⁷⁻³⁹. WT B6 mice were injected with MAR1-5A3 antibody or PBS one day prior to inoculation with D220 virus. On the following day (Day 0), mice were immunized with either OVA mRNA-LNP or control eGFP mRNA-LNP. Seven days post-immunization, vaccine-specific CD8⁺ T cell responses were assessed (Fig. 7A). We tracked weight of these mice throughout the experiment and saw no changes between mock infected and infected mice (Fig. 7B). We found that mice infected with D220, had a significant reduction in vaccine-specific CD8⁺ T cells populations compared to mock infected mice (Fig. 7C). Mice injected with MAR1-5A3 antibody had equivalent vaccine-specific CD8⁺ T cell populations when compared to unblocked mice (Fig. 7C). However, IFN α R blockade in D220-infected mice resulted in increased PD-1 expression compared to both uninfected mice and unblocked D220-infected mice (Fig. 7D). Dengue infection is known to produce other inflammatory cytokines such as TNF α , IL-6, and IL-1 β ³⁷⁻³⁹ which can activate DCs and decrease their ability to acquire the mRNA-LNP vaccine.

Thus, inhibiting IFN α R signaling alone in an infection model may not be sufficient to restore the response. However, in contexts where IFN is produced in isolation, such as with mRNA-based vaccines, IFN α R blockade can be effective.

Vaccine-specific CD8 $^{+}$ T cells produced in setting of IFN α R blockade display increased ability to control tumors

It has been shown that lack of IFN α R expression on CD8 $^{+}$ T cells abrogates their cytolytic ability¹³. Therefore, while we see an increase in vaccine-specific CD8 $^{+}$ T cells, it is possible that IFN α R blockade could inhibit their cytolytic capacity. To assess whether IFN α R inhibition altered CD8 $^{+}$ T cell function, we used an *in vivo* T cell cytotoxicity assay that monitored the capacity of naturally arising CTLs to kill peptide-pulsed splenocytes labelled with cell trace violet (CTV). WT C57BL/6J IFN α R blocked and unblocked mice immunized with OVA mRNA-LNP vaccines equivalently killed CTV^{hi}-labelled SIINFEKL peptide-pulsed splenocytes but not CTV^{lo}-labelled irrelevant peptide-pulsed splenocytes 10 days following immunization (Fig. 8A). In contrast, WT C57BL/6J mice immunized with eGFP mRNA-LNP were incapable of eliminating both CTV^{hi}-labelled SIINFEKL peptide-pulsed splenocytes and CTV^{lo}-labelled irrelevant peptide-pulsed splenocytes (Fig. 8A). Next, we tested if IFN α R blockade influenced inflammatory cytokine production. We found that blocking IFN α R prior to immunization did not alter production of IFN γ in vaccine-specific CD8 $^{+}$ T cells (Fig. 8B). Thus, IFN α R blockade did not diminish the effector capacity of vaccine-elicited CD8 $^{+}$ T cells.

To further investigate the function of vaccine-induced CD8⁺ T cells generated when IFN α R is inhibited, we used the B16F10 melanoma model engineered to express membrane-bound ovalbumin (B16 mOVA, Supplementary Fig. 5)⁴⁰. WT B6 mice were injected intraperitoneally with MAR1-5A3 antibody or PBS and then immunized with either OVA or eGFP mRNA-LNP vaccines the following day. Fourteen days later, B16-mOVA tumor cells were implanted subcutaneously into the flank and were followed for tumor growth (Fig. 8C). As expected, mice immunized with the control eGFP mRNA-LNP failed to reject tumors (Fig. 8D). Mice immunized with OVA mRNA-LNP alone displayed delayed outgrowth; some tumors progressed indicating that the vaccine-induced CD8⁺ T cell response was insufficient to maintain tumor control. In contrast, mice treated with IFN α R-blocking antibody showed sustained control of B16-mOVA tumors over the course of the experiment, suggesting that CD8⁺ T cells generated in the absence of IFN α R signaling had an enhanced capacity to control tumor growth. (Fig. 8D).

Discussion

Type I interferons are produced upon sensing of viral products such as viral RNA or DNA and induce many antiviral interferon-stimulated genes (ISGs)¹². For instance, IFN activate Protein Kinase R (PKR), which phosphorylates eukaryotic initiation factor 2 α (eIF2 α). This phosphorylation halts cap-dependent translation, leading to a global shutdown of protein synthesis in infected and neighboring cells to prevent viral replication⁴¹. Additionally, IFN signaling induces 2',5'-oligoadenylate synthetase (OAS) and RNase L, which degrade cellular and viral RNA, further suppressing translation⁴¹. In

addition, it has been shown that an activated DC loses its ability to acquire new material^{21,23}. Because IFN activates DCs and induces a myriad of ISGs inhibiting transcription and translation, APCs that sense IFN could be blunted in their ability to acquire and/or translate mRNA-LNPs. Indeed, APCs that were activated before exposure to FITC-dextran were unable to internalize it²¹. Similarly, systemic malaria infection severely inhibited antigen cross-presentation by DCs, in agreement with our hypothesis²². On the other hand, when DCs are stimulated by IFN, they upregulate several co-stimulatory molecules that enhance T cell activation. Key costimulatory molecules such as CD80 (B7-1), CD86 (B7-2), and CD40 promote T cell priming, expansion, and cytokine production. Additionally, IFN stimulation increases the expression of MHC class I and II, enhancing antigen presentation to CD8⁺ and CD4⁺ T cells, respectively^{12,15,42}. Together, these co-stimulatory molecules enhance T cell priming and activation, linking innate immune sensing with adaptive immune responses. These contrasting roles of IFN are possibly why many studies seem to show opposing effects on the adaptive immune response when IFN is present. We propose that IFN primarily evolved as a mechanism to inhibit viral replication and dissemination and secondarily within APCs to enhance adaptive immunity. However, the *timing* of IFN sensing is critical in determining its impact on immune responses. IFN signaling in APCs during antigen acquisition can help limit viral replication while still allowing the APCs to acquire and present antigens. If IFN signaling occurs during antigen uptake, APCs can effectively process and present viral antigens while simultaneously initiating antiviral defenses. However, if IFN is sensed after a period before the virus or antigen is acquired, the APC diverts to inhibiting viral dissemination. This is accomplished by

inhibiting additional antigen uptake and shutting down translation ensuring the DC presents material already acquired, thereby preventing the virus from replicating and spreading systemically. Thus, IFN functions in a delicate balance between antiviral defense and immune activation, with its timing shaping the overall effectiveness of the innate antigen presentation response. During vaccination, the primary goal is to maximize the spread and uptake of the vaccine by as many APCs as possible. In this context, IFN signaling within APCs can be detrimental, as it may suppress antigen acquisition and/or mRNA-LNP translation. Here we show that inhibiting IFN signaling enhances the ability of more APCs to take up, translate, and process the vaccine, leading to a more effective immune response. Since mRNA-LNPs are already potent stimulators of APCs through pattern recognition receptor (PRR) activation^{6,10}, the additional immune stimulation provided by IFN signaling is unnecessary and hinders optimal vaccine efficacy as we have shown herein.

We have demonstrated that when mRNA-LNPs are targeted to APCs, that IFN signaling inhibits adaptive immune responses. However, it should be noted that different formulations of LNPs could potentially target different cell types and locations. Indeed, it has been shown that altering the cationic ratio of mRNA to LNP, targets LNPs to different organs⁶. Our mRNA-LNP targets the spleen and to APCs in particular. Therefore, inhibiting IFN signaling allows for more mRNA-LNP acquisition. If an mRNA-LNP vaccine were designed to exclusively target fibroblasts or epithelial cells, IFN signaling within DCs may be necessary for recognizing the vaccine as foreign. In this scenario, since DCs would not be directly activated through PRR signaling, they might rely on IFN signaling from mRNA-LNP expressing cells to enhance antigen presentation

and stimulate the adaptive immune response. Given that mRNA-LNP vaccines are still a relatively new technology, it is essential to investigate how different LNP formulations are distributed and sensed across various cell types. Understanding this distribution could help refine strategies for modulating IFN signaling, potentially identifying opportunities to inhibit IFN where it may be detrimental or leverage it where it is beneficial.

Our results also suggest that immunization during an ongoing immune response is detrimental. We found that administering a vaccine too soon, either during an ongoing infection or shortly after a different vaccination, significantly diminished the immune response to the new vaccine. In the case of two mRNA-LNP vaccines administered just one day apart, the diminished immune response appeared to be at least partially due to premature IFN activation of DCs, impairing their ability to acquire and express the second vaccine. This was supported by our finding that transient IFN α R blockade rescued the adaptive immune response. However, when Dengue virus infection was followed the next day by mRNA-LNP vaccination, the reduction in vaccine-specific immunity could not be rescued by IFN α R blockade. This suggests that mRNA-LNP immunizations following an infection cannot be rescued by inhibiting IFN signaling alone. Indeed, it has been shown that dengue infection induces a low but systemic TNF α response³⁷, which could activate DCs and prevent them from effectively processing the subsequent mRNA-LNP vaccine. These findings highlight the importance of timing in vaccination strategies and describe a mechanistic hypothesis for the reduced response to vaccines when infected. Administering vaccines too closely

together or during an ongoing infection, even if asymptomatic, can significantly impair vaccine efficacy by disrupting antigen presentation and adaptive immune priming. While our results are primarily focused on the CD8⁺ T cell response, we did not see changes in the CD4⁺ T cell response. MAR1-5A3 administration did improve CD4⁺ T cell response by percentage of TCR β ⁺CD4⁺CXCR5⁺PD-1⁺B220⁻ T follicular helper (Tfh) cells (Supplementary Fig. 6). Our model proved to mainly be a CD8⁺ T cell effect which still demonstrates an important effect that can be used for mRNA-LNP vaccine development.

Finally, our results demonstrate that transient blockade of IFN α R signaling does not compromise, but enhances, the cytotoxic capacity of the vaccine-specific CD8⁺ T cell response, contrary to previously published reports^{13,43}. When vaccinated mice were injected with vaccine-specific peptide-pulsed splenocytes, they exhibited cytotoxic T cell responses that were comparable to those of controls. Additionally, IFN α R blocked vaccine-specific CD8⁺ T cells displayed enhanced protection against tumor outgrowth. Thus, in the context of mRNA-LNP vaccination against patient-specific neoantigens, inhibiting IFN α R signaling transiently could potentially augment neoantigen elicited CD8⁺ T cell responses and lead to better tumor control. Altogether, our findings reveal that IFN signaling plays a context and timing dependent role in shaping the immune response to mRNA-LNP vaccines. These insights provide a compelling rationale for optimizing vaccine schedules and formulation strategies to transiently modulate innate signaling pathways, particularly IFN α R, to maximize antigen acquisition, mRNA expression, T cell priming, and therapeutic efficacy.

Methods

Study Design

This study aimed to determine the role of type 1 interferon signaling on DCs in the process of creating an adaptive immune response to mRNA-LNP vaccines. We hypothesized that early IFN signaling within DCs impairs their ability to acquire new antigenic material, thereby limiting antigen presentation and ultimately leading to a diminished adaptive immune response. We used a combination of in vitro experiments using bone marrow derived dendritic cells as well as in vivo experiments using a variety of mouse models that are described in each respective results section. We inhibited type 1 interferon signaling in various ways as well as administering mRNA-LNP to cells and mice to then measure adaptive immune responses by flow cytometry. This was used to determine the ability to acquire mRNA-LNP and create a strong adaptive immune response to the antigen in question. No randomization was done, and blinding was not necessary as most data was quantified by objective readouts by flow cytometry. Sample sizes were determined by previous experiments, and the number of biological replicates are indicated by “n” in each figure legend. Each experiment was replicated at least once with consistent results. Outliers were defined by a ROUT test with $Q=1\%$. One outlier was determined and excluded in the study under Figure 4 within the OVA group.

Mice

WT C57BL/6J (Jax stock no. 000664), CD11c^{Cre} mice (stock no. 008068), IFN α R^{fl/fl} mice (stock no. 028256), Zeb2 triple enhancer mutant mice (Δ 1, 2, 3; stock

no. 037704), and cD11c DTR mice (stock no. 004509) mice were purchased from The Jackson Laboratory and bred in-house. *Irf8* +32^{-/-} ($\Delta 32$) mice, which are homozygous for the deletion of a downstream enhancer element of *Irf8*, were gifted by Dr. Kenneth Murphy at Washington University in St. Louis and described previously³². All mice were housed under a 12-h dark/light cycle, and housing was maintained at an ambient temperature of 72°F. Mice were age-matched and sex-matched and between 8 and 16 weeks of age when used for experiments. Mice were humanely euthanized by CO₂ anesthesia followed by cervical dislocation in accordance with the Guide for the Care and Use of Laboratory Animals of the NIH under approval by the Institutional Animal Care and Use Committee (IACUC) at Saint Louis University School of Medicine (Assurance Number: D16-00141).

mRNA and LNP generation

The DNA plasmid used for in vitro transcription was based on a previously published Zika virus vaccine design (PMC5388441). Briefly, the gene of interest (GOI) was flanked by a 5' untranslated region (UTR; 5'-

GGGAAATAAGAGAGAAAAGAAGAGTAAGAAGAAATATAAGAGGCCACC-3') and a 3'

UTR (5'-

TAATAGGCTGGAGCCTCGGTGCCATGCTTCTGCCCTGGCCTCCCCCAGC
CCCTCCTCCCCCTTCCTGCACCCGTACCCCGTGGTCTTGAATAAGTCTGA-3'),

followed by a poly(A) tail consisting of 120 adenosines with a single guanosine interruption in the middle. The GOI was cloned into a multiple cloning site without a secretion signal sequence. The expression vector includes the T7 Promoter, 5' and 3'

untranslated region (UTR) flanking the ZsGreen1, eGFP, or cytosolic Ovalbumin (OVA), and the AG CleanCap nucleotide sequence after the TATA box sequence for downstream *in vitro* mRNA transcription. The plasmid was transformed into DH5a competent *E. coli* cells (NEB Cat No. C2988J) and plated onto Ampicillin agar plates for resistant colonies to grow. Colonies were harvested and checked for correct insert size by colony PCR and sequenced. Correct plasmids were grown in 250 mL LB ampicillin cultures and purified via endotoxin free plasmid maxi kits (Qiagen Cat No. 12362). After plasmid purification, the plasmid was digested using the restriction enzymes BgIII and Xhol at 37°C overnight. The insert was isolated via gel purification using Gel/PCR DNA fragments extraction kits (IBI scientific cat IB47020). These fragments were used for *in vitro* mRNA transcription via mRNA Kit with CleanCap Reagent AG (NEB Cat No. E2080S) utilizing CleanCap for the 5' cap and pseudo-uridine in place of uridine as per manufacturers protocol, and left overnight at 37°C. Encapsulation of the mRNA was performed on a NanoAssemblr Ignite Instrument (Cat No. NIN0001). The mRNA was dissolved in PNI Formulation Buffer (Cat No. NWW0043) and run through a NanoAssemblr Ignite NxGen Cartridge (Cat No. NIN0061) with the lipid nanoparticle GenVoy ILM or GenVoy-ILM with Dye formulations (Cat No. NWW0042) at a flow ratio of 3:1 and a total flow rate of 12 mL/min to generate the LNP encapsulated mRNA vaccines. For downflow processing, the size of the LNP particles was determined by polydispersity index (PDI) by Dynamic Light Scattering (DLS). The mRNA-LNPs were subsequently concentrated and purified by diluting the samples in PBS and filtrating via centrifugal filtration using a filtration tube (Millipore Sigma Amicon Ultra-15 Cat No. C7715). Measurement of the mRNA concentration within the LNP and encapsulation

efficiency was performed using a Quant-IT RiboGreen Assay (Thermo Fisher Scientific Cat No. R11490).

In vitro DC cultures

Bone marrow (BM) was harvested from femurs and tibias from WT C57BL/6J mice. Bones were crushed with a mortar and pestle in Iscove's modified Dulbecco's media (IMDM) supplemented with 10% FCS (Gibco) and were passed through 70- μ m filters. Red blood cells were lysed using ammonium chloride-potassium bicarbonate (ACK) buffer. After RBC lysis, cells were brought up in I10F, counted via the Countess-3 (Fisher) cell counter. Cells were then plated at 10^5 cells/mL in I10F supplemented with 10% SCF conditioned media for 3 days. Cells were then washed in I10F and replated and cultured in I10F supplemented with 5% Flt3L-Fc conditioned media for 8 days. On day 6 of Flt3L-Fc culture, some DCs were cultured with recombinant IFN α at 10^3 U/mL for 16 hours prior to receiving mRNA-LNP. On Day 7, DCs were cultured with 2.5 ug ZsGreen or eGFP mRNA-LNP with or without 10 ug MAR1-5A3 anti-IFN α R blocking antibody and cultured for 24 hours. At 24 hours following mRNA-LNP addition, cells were harvested and stained with fluorescently labeled antibodies at 4°C in magnetic-activated cell-sorting (MACS) buffer (PBS + 0.5% BSA + 2 mM EDTA) in the presence of 10% Fc block supernatant from 2.4G2 cells and analyzed via flow cytometry.

CD8 $^+$ T cell Tetramer Staining

Spleens were harvested at different timepoints indicated by each experiment respectively. Whole spleens were mashed and digested in collagenase B (250mg/mL)

and DNase (10mg/mL) in Iscove's modified Dulbecco's media (IMDM) supplemented with 10% FCS (Gibco) for 45 minutes at 37°C with shaking. Red blood cells were lysed with ammonium chloride–potassium bicarbonate (ACK) lysis buffer. Cells were subsequently counted with a Countess 3 (Invitrogen). SIINFEKL-H2-K^b biotinylated monomers were purchased from the NIH. Then, the peptide–MHC multimers were incubated with PE- and APC-conjugated streptavidin (SA) at a concentration of 1:9 for 30 min at 4°C protected from light in separate reactions. SA-labelled tetramers were then incubated with 25 µM D-biotin for 20 min at 4 °C protected from light to quench free fluorochrome-labelled SA. 3×10^6 splenocytes were incubated in MACS buffer containing the Fc-blocking antibody produced from the 2.4G2 cell line for 5 min at 4 °C. Fluorochrome-conjugated tetramers were added to the splenocytes at a concentration of 1:50 and incubated at 4°C for 30 min. Surface antibodies were added without washing and stained for another 30 min at 4°C.

Antibodies and flow cytometry

Flow cytometry was completed on a FACS Cantoll (BD) and analyzed using FlowJo analysis software (Tree Star). Staining was performed at 4°C in the presence of Fc block (10% 2.4G2 supernatant) in MACS buffer. The following antibodies were used; from Biolegend: KLRG1 (clone: 2F1/KLRG1), CD45.1 (clone: A20), MHCII (clone: M5/114.15.2), IFN α R (clone: MAR1-5A3), CD40 (clone: FGK45), V α 2 (clone: B20.1), Sirp α (clone: P84), CD45.2 (clone: 104), TCR β (clone: H57-597), PD-1 (clone: 29F.1A12), CD86 (clone: GL-1), Ly6C (clone: HK1.4), CD4 (clone: Rm4-5), CD44 (clone: IM7), CD11c (clone: N418), XCR1 (clone: ZET), B220 (clone: RA3-6B2), CD8 α

(clone: 53-6.7), IL-7R α (clone: A7R34), F4/80 (clone: BM8), IFN γ (clone: XMG1.2), CXCR5 (clone: L138D7), PE streptavidin (cat: 405204), and APC streptavidin (cat: 405207). The anti-OVA antibody was purchased from Millipore (Millipore AB1225).

Mice Immunizations

The blocking α IFN α R antibody (MAR1-5A3; Leinco) was administered to mice at 250ug intraperitoneally (IP). Blocking IFN α R with MAR1-5A3 occurred one day before immunizing with mRNA-LNP. OVA mRNA-LNP was immunized in mice at 2.5ug intravenously (IV) through the tail vein. ZsGreen or eGFP mRNA-LNP was immunized at either 5ug or 2.5ug intravenously through the tail vein indicated by each experiment respectively. We labeled all experiments that used ZsGreen or eGFP mRNA-LNP as just eGFP mRNA-LNP to conserve space. There was no difference seen between these different constructs.

ELISA

For IFN α ELISA, whole serum was isolated from mice at hour 0 before immunization as well as hours 8 and 24 post mRNA-LNP vaccination. Whole serum was stored at -80°C and was analyzed for IFN α 2 and 4 with an IFN alpha ELISA KIT (Invitrogen: Cat. BMS6027).

Dengue Infection

WT C57BL/6J mice were used in the Dengue infection studies. Mice were administered with 250 μg MAR1-5A3 antibody intraperitoneally, one day before being infected with a

mouse adapted dengue virus strain grown in C6/26 cells (D220, a gift from Eva Harris, UC Berkeley)⁴⁴. Infections were performed intramuscularly into the hind leg of the mouse with 6.5×10^6 FFU per mouse. One day post-infection, mice were immunized with mRNA-LNP at 2.5ug intravenously. Body weight was recorded every other day until the mice were sacrificed on day 7 post mRNA-LNP immunization.

Tumor line and growth experiment

The tumor line used was the B16F10 melanoma membrane expressing ovalbumin (B16-mOVA). The B16-mOVA line was engineered to express membrane ovalbumin (mOVA) using a MSCV-mOVA-IRES-Thy1.1 vector as previously described⁴¹. B16F10 tumor cells were retrovirally transduced with a pMSCV vector expressing mOVA (B16mOVA; Fig. 8). Clone 2 was selected by expression of surface OVA (Millipore AB1225) using flow cytometry. WT C57BL/6J mice were either given 250ug MAR1-5A3 antibody intraperitoneally or PBS then immunized with 2.5ug of OVA mRNA-LNP intravenously a day later. Control mice were immunized with 2.5ug of eGFP mRNA-LNP. Fourteen days post immunization, mice were subcutaneously injected with 10^6 B16mOVA tumor cells into the flank. Tumor growth was measured with a caliper, and tumor area was calculated by the multiplication of two perpendicular diameters. Growth measurements were taken on days 0, 4, 7, 11, 14, 18, and 21 post inoculation. In accordance with our IACUC-approved protocol, maximal tumor diameter was 20 mm in one direction, and in no experiments was this limit exceeded.

Intracellular Interferon gamma stain

Spleens were harvested 7 days post mRNA-LNP immunization. Whole spleens were mashed and digested in collagenase B (250mg/mL) and DNase (10mg/mL) in Iscove's modified Dulbecco's media (IMDM) supplemented with 10% FCS (Gibco) for 45 minutes at 37°C with shaking. Red blood cells were lysed with ammonium chloride–potassium bicarbonate (ACK) lysis buffer. Cells were subsequently counted with a Countess 3 (Invitrogen). Cells were then incubated with Brefeldin A (BFA)(10ug/mL) and SIINFEKL-H2-K^b (10uM), or BFA with irrelevant peptide for 5hr at 37°C. Cells were then stained normally at 4°C for 30min for surface antibodies. Cells were then washed before being fixed with the FoxP3 Fix/Perm Buffer set (Biolegend 421403) for 20min at room temperature. Then cells were stained with intracellular antibody IFN γ in perm buffer at 4°C for 1hr. Cells were then washed once with perm buffer and once with MACS buffer before being used for flow cytometry.

Statistical Analysis

Statistical analysis was performed using GraphPad Prism software version 10. Unless otherwise noted, a one-way ANOVA, Unpaired two-tailed Students T test, or Mann–Whitney test was used to determine significant differences between samples, and all center values correspond to the mean. $P \leq 0.05$ was considered statistically significant. Investigators were blinded to the treatments of the mice during sample preparation and data collection.

Data availability

All data generated or analyzed during this study are included in this published article and its supplementary information files.

Acknowledgments

Stephen T. Ferris is supported by the President's Research Fund of Saint Louis University School of Medicine (S.F.). Elise Alspach, PhD, is supported by a Research Scholar Grant, RSG-24-1251974-01-IBCD, from the American Cancer Society (<https://doi.org/10.53354/ACS.RSG-24-1251974-01-IBCD.pc.gr.193734>), and is the recipient of a Cancer Research Institute CLIP Grant (CRI5509). We thank the NIH Tetramer Core Facility (NIH Contract 75N93020D00005 and RRID:SCR_026557) for providing H2-K^b chicken ova 257-264 SIINFEKL Monomer.

Author Contributions

Conceptualization: STF, TAL, AD

Methodology: STF, TAL, EA, LVT

Investigation: TAL, STF, SB, JAC, YD, WG

Visualization: TAL, STF

Funding acquisition: STF

Project administration: STF, RJD

Supervision: STF

Writing – original draft: TAL, STF

Writing – review & editing: TAL, STF, EA, LVT, WG

Competing Interest

All authors declare no competing interests.

References

1. Arevalo, C. P. *et al.* A multivalent nucleoside-modified mRNA vaccine against all known influenza virus subtypes. *Science* **378**, 899–904 (2022).
2. Xie, Z. *et al.* mRNA-LNP HIV-1 trimer boosters elicit precursors to broad neutralizing antibodies. *Science* **384**, eadk0582 (2024).
3. Barbier, A. J., Jiang, A. Y., Zhang, P., Wooster, R. & Anderson, D. G. The clinical progress of mRNA vaccines and immunotherapies. *Nat. Biotechnol.* **40**, 840–854 (2022).
4. Rojas, L. A. *et al.* Personalized RNA neoantigen vaccines stimulate T cells in pancreatic cancer. *Nature* **618**, 144–150 (2023).
5. Liu, C. *et al.* mRNA-based cancer therapeutics. *Nat. Rev. Cancer* **23**, 526–543 (2023).
6. Kranz, L. M. *et al.* Systemic RNA delivery to dendritic cells exploits antiviral defence for cancer immunotherapy. *Nature* **534**, 396–401 (2016).
7. Sethna, Z. *et al.* RNA neoantigen vaccines prime long-lived CD8+ T cells in pancreatic cancer. *Nature* **639**, 1042–1051 (2025).
8. Sittplangkoon, C. *et al.* mRNA vaccine with unmodified uridine induces robust type I interferon-dependent anti-tumor immunity in a melanoma model. *Front. Immunol.* **13**, 983000 (2022).

9. Arunachalam, P. S. *et al.* Systems vaccinology of the BNT162b2 mRNA vaccine in humans. *Nature* **596**, 410–416 (2021).
10. Li, C. *et al.* Mechanisms of innate and adaptive immunity to the Pfizer-BioNTech BNT162b2 vaccine. *Nat. Immunol.* **23**, 543–555 (2022).
11. Kim, S. *et al.* Innate immune responses against mRNA vaccine promote cellular immunity through IFN- β at the injection site. *Nat. Commun.* **15**, 7226 (2024).
12. McNab, F., Mayer-Barber, K., Sher, A., Wack, A. & O'Garra, A. Type I interferons in infectious disease. *Nat. Rev. Immunol.* **15**, 87–103 (2015).
13. Kolumam, G. A., Thomas, S., Thompson, L. J., Sprent, J. & Murali-Krishna, K. Type I interferons act directly on CD8 T cells to allow clonal expansion and memory formation in response to viral infection. *J. Exp. Med.* **202**, 637–650 (2005).
14. Sikora, A. G. *et al.* IFN- α Enhances Peptide Vaccine-Induced CD8+ T Cell Numbers, Effector Function, and Antitumor Activity. *J. Immunol.* **182**, 7398–7407 (2009).
15. Ngai, S. M., Tovey, M. G. & Vella, A. T. Targeting Poly I:C to the TLR3-independent pathway boosts effector CD8 T cell differentiation through IFN α / β . *J. Immunol. Baltim. Md 1950* **181**, 7670–7680 (2008).
16. Hall, J. C. & Rosen, A. Type I interferons: crucial participants in disease amplification in autoimmunity. *Nat. Rev. Rheumatol.* **6**, 40–49 (2010).
17. Su, A. I. *et al.* Genomic analysis of the host response to hepatitis C virus infection. *Proc. Natl. Acad. Sci. U. S. A.* **99**, 15669–15674 (2002).
18. O'Garra, A. *et al.* The immune response in tuberculosis. *Annu. Rev. Immunol.* **31**, 475–527 (2013).

19. McNab, F. W. *et al.* TPL-2-ERK1/2 signaling promotes host resistance against intracellular bacterial infection by negative regulation of type I IFN production. *J. Immunol. Baltim. Md 1950* **191**, 1732–1743 (2013).
20. Berry, M. P. R. *et al.* An interferon-inducible neutrophil-driven blood transcriptional signature in human tuberculosis. *Nature* **466**, 973–977 (2010).
21. Sallusto, F., Cella, M., Danieli, C. & Lanzavecchia, A. Dendritic cells use macropinocytosis and the mannose receptor to concentrate macromolecules in the major histocompatibility complex class II compartment: downregulation by cytokines and bacterial products. *J. Exp. Med.* **182**, 389–400 (1995).
22. Wilson, N. S. *et al.* Systemic activation of dendritic cells by Toll-like receptor ligands or malaria infection impairs cross-presentation and antiviral immunity. *Nat. Immunol.* **7**, 165–172 (2006).
23. Theisen, D. J. *et al.* Batf3-Dependent Genes Control Tumor Rejection Induced by Dendritic Cells Independently of Cross-Presentation. *Cancer Immunol. Res.* **7**, 29–39 (2019).
24. Sheehan, K. C. F. *et al.* Blocking monoclonal antibodies specific for mouse IFN-alpha/beta receptor subunit 1 (IFNAR-1) from mice immunized by in vivo hydrodynamic transfection. *J. Interferon Cytokine Res. Off. J. Int. Soc. Interferon Cytokine Res.* **26**, 804–819 (2006).
25. Palacio, N. *et al.* Early type I IFN blockade improves the efficacy of viral vaccines. *J. Exp. Med.* **217**, e20191220 (2020).

26. Bullock, C. B. *et al.* Type I interferon signaling in dendritic cells limits direct antigen presentation and CD8+ T cell responses against an arthritogenic alphavirus. *mBio* **15**, e02930-24 (2024).

27. Broomfield, B. J. *et al.* Transient inhibition of type I interferon enhances CD8+ T cell stemness and vaccine protection. *J. Exp. Med.* **222**, (2025).

28. Ou, F. *et al.* Enhanced in vitro type 1 conventional dendritic cell generation via the recruitment of hematopoietic stem cells and early progenitors by Kit ligand. *Eur. J. Immunol.* **53**, e2250201 (2023).

29. Ryman, K. D. *et al.* Sindbis Virus Translation Is Inhibited by a PKR/RNase L-Independent Effector Induced by Alpha/Beta Interferon Priming of Dendritic Cells. *J. Virol.* **79**, 1487–1499 (2005).

30. Ahn, E. *et al.* Role of PD-1 during effector CD8 T cell differentiation. *Proc. Natl. Acad. Sci.* **115**, 4749–4754 (2018).

31. Zahm, C. D., Colluru, V. T. & McNeel, D. G. Vaccination with High-Affinity Epitopes Impairs Antitumor Efficacy by Increasing PD-1 Expression on CD8+ T Cells. *Cancer Immunol. Res.* **5**, 630–641 (2017).

32. Zheng, L., Bandara, S. R., Tan, Z. & Leal, C. Lipid nanoparticle topology regulates endosomal escape and delivery of RNA to the cytoplasm. *Proc. Natl. Acad. Sci.* **120**, e2301067120 (2023).

33. Caton, M. L., Smith-Raska, M. R. & Reizis, B. Notch-RBP-J signaling controls the homeostasis of CD8- dendritic cells in the spleen. *J. Exp. Med.* **204**, 1653–1664 (2007).

34. Prigge, J. R. *et al.* Type-I-IFNs act upon hematopoietic progenitors to protect and maintain hematopoiesis during *Pneumocystis* lung infection in mice. *J. Immunol. Baltim. Md 1950* **195**, 5347–5357 (2015).

35. Durai, V. *et al.* Cryptic activation of an *Irf8* enhancer governs cDC1 fate specification. *Nat. Immunol.* **20**, 1161–1173 (2019).

36. Liu, T.-T. *et al.* Ablation of cDC2 development by triple mutations within the *Zeb2* enhancer. *Nature* <https://doi.org/10.1038/s41586-022-04866-z> (2022) doi:10.1038/s41586-022-04866-z.

37. Shresta, S., Sharar, K. L., Prigozhin, D. M., Beatty, P. R. & Harris, E. Murine Model for Dengue Virus-Induced Lethal Disease with IncreasedVascular Permeability. *J. Virol.* **80**, 10208–10217 (2006).

38. Chen, H.-W. *et al.* The Roles of IRF-3 and IRF-7 in Innate Antiviral Immunity against Dengue Virus. *J. Immunol.* **191**, 4194–4201 (2013).

39. Chen, H.-C., Hofman, F. M., Kung, J. T., Lin, Y.-D. & Wu-Hsieh, B. A. Both Virus and Tumor Necrosis Factor Alpha Are Critical for Endothelium Damage in a Mouse Model of Dengue Virus-Induced Hemorrhage. *J. Virol.* **81**, 5518–5526 (2007).

40. Ferris, S. T. *et al.* cDC1 prime and are licensed by CD4+ T cells to induce anti-tumour immunity. *Nature* <https://doi.org/10.1038/s41586-020-2611-3> (2020) doi:10.1038/s41586-020-2611-3.

41. Yan, N. & Chen, Z. J. Intrinsic antiviral immunity. *Nat. Immunol.* **13**, 214–222 (2012).

42. Busselaar, J., Sijbranda, M. & Borst, J. The importance of type I interferon in orchestrating the cytotoxic T-cell response to cancer. *Immunol. Lett.* **270**, 106938 (2024).

43. Li, C. *et al.* Mechanisms of innate and adaptive immunity to the Pfizer-BioNTech BNT162b2 vaccine. *Nat. Immunol.* **23**, 543–555 (2022).

44. Orozco, S. *et al.* Characterization of a model of lethal dengue virus 2 infection in C57BL/6 mice deficient in the alpha/beta interferon receptor. *J. Gen. Virol.* **93**, 2152–2157 (2012).

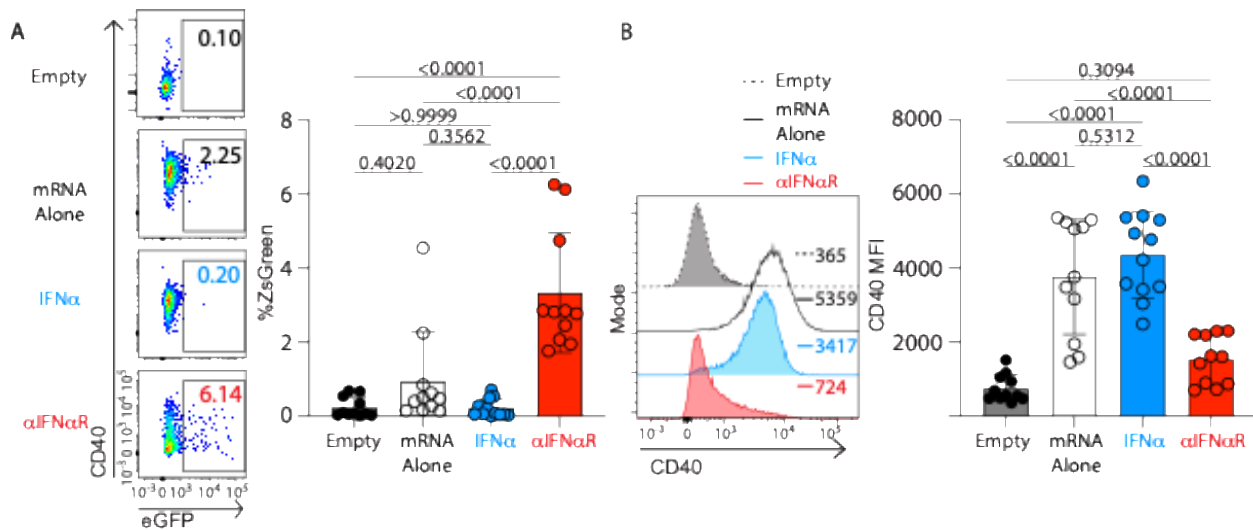


Figure 1. mRNA-LNP vaccine induced IFN reduces overall mRNA uptake by DCs *in vitro*.

(A) (Left) Representation flow plots of eGFP expression of BMDCs incubated with 2.5ug eGFP mRNA-LNP alone, with mRNA-LNP and MAR1-5A3 antibody (α IFN α R, red), or with mRNA-LNP and 10³ U/mL IFN α for 16 hours (blue). (Right) eGFP expression as a percentage of all DCs incubated with 2.5ug eGFP mRNA-LNP alone (white), with mRNA-LNP and MAR1-5A3 antibody (α IFN α R, red), or with mRNA-LNP and 10³ U/mL IFN α for 16 hours (blue). **(B)** (Left) Representative flow plots of CD40 MFI of BMDCs incubated with 2.5ug eGFP mRNA-LNP alone, with mRNA-LNP and MAR1-5A3 antibody (α IFN α R, red), or with mRNA-LNP and 10³ U/mL IFN α for 16 hours (blue). (Right) CD40 MFI of DCs incubated with 2.5ug eGFP mRNA-LNP alone (white), with mRNA-LNP and MAR1-5A3 antibody (α IFN α R, red), or with mRNA-LNP and 10³ U/mL IFN α for 16 hours (blue). Data represents pooled independent samples from four independent experiments (n=11 for empty, n=11 for mRNA alone, n=12 for IFN α , and n=11 for α IFN α R). Data were compared using one-way ANOVA.

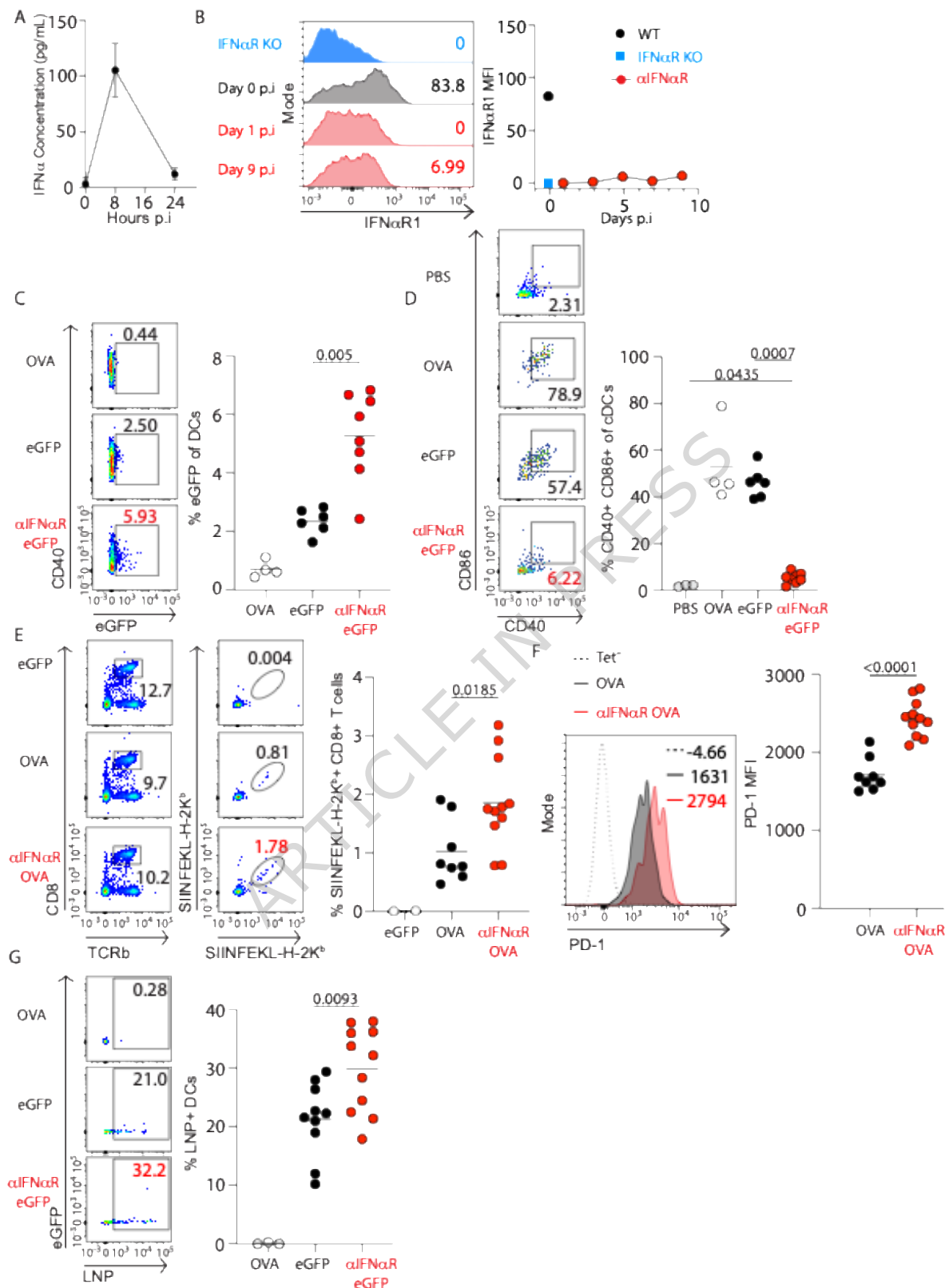


Figure 2. IFN α R Blockade increases vaccine-specific CD8 $^{+}$ T cell responses.

(A) Serum levels of IFN α 2 and 4 at various timepoints after immunization with 2.5ug of mRNA-LNP from four C57BL/6J wildtype mice (WT) pooled together. **(B)** (Left) Surface expression of IFN α R1 from mice given 250ug of MAR1-5A3 (α IFN α R, red) (IP), or no MAR1-5A3 (black) and compared to an IFN α R knockout mouse (blue). (Right) Representative plot showing IFN α R1 MFI of each mouse at days 1, 3, 5, 7, and 9 post injection of MAR1-5A3 (red, n=5) compared to a WT mouse with no MAR1-5A3 injection (black, n=1) or an IFN α R knockout mouse (blue, n=1). **(C)** (Left) Representative flow plot of splenic cD11c $^+$ MHCII $^+$ DCs expressing eGFP from WT mice with or without MAR1-5A3. (Right) Percentage of eGFP expression in splenic DCs 24hr post mRNA-LNP immunization (5ug eGFP mRNA-LNP or 2.5ug OVA mRNA-LNP IV) in WT mice (black, n=6), or WT mice given MAR1-5A3 prior to immunization (red, n=8). **(D)** (Left) Representative flow plot showing CD40 $^+$ CD86 $^+$ splenic DCs after immunization with mRNA-LNP with or without MAR1-5A3. (Right) Percentage of CD40 $^+$ CD86 $^+$ splenic DCs from mice in Fig. 2C. **(E)** (Left) Representative flow plots of SIINFEKL-H2-K b (OVA) specific CD8 $^+$ T cells. (Right) Percentage of OVA specific CD8 $^+$ T cells from WT mice (black, n=8) and WT mice given MAR1-5A3 (red, n=11). 2.5ug of mRNA-LNP was administered IV 24hr after MAR1-5A3. **(F)** (Left) Representative flow plot showing PD-1 expression of OVA specific TCR β $^+$ CD8 α $^+$ T cells. (Right) PD-1 expression of TCR β $^+$ CD8 α $^+$ T cells from mice in Fig. 2E. **(G)** (Left) Representative flow plot of splenic cD11c $^+$ MHCII $^+$ DCs expressing fluorescent LNP from WT mice with or without MAR1-5A3. (Right) Percentage of LNP expression in splenic DCs 24hr post mRNA-LNP immunization (5ug DiD incorporated LNP eGFP mRNA-LNP or 2.5ug OVA mRNA-LNP IV) in WT mice (black, n=10), or WT mice given MAR1-5A3 prior to immunization (red,

n=11). Error bars in (A) indicate \pm SD. All bars in (C)-(G) indicate the mean. Data in (C) and (E) were compared using a Mann Whitney test. Data in (D) were compared with either an unpaired two tailed students T test or a Mann Whitney test. Data in (F) and (G) were compared by an unpaired two tailed students T test.

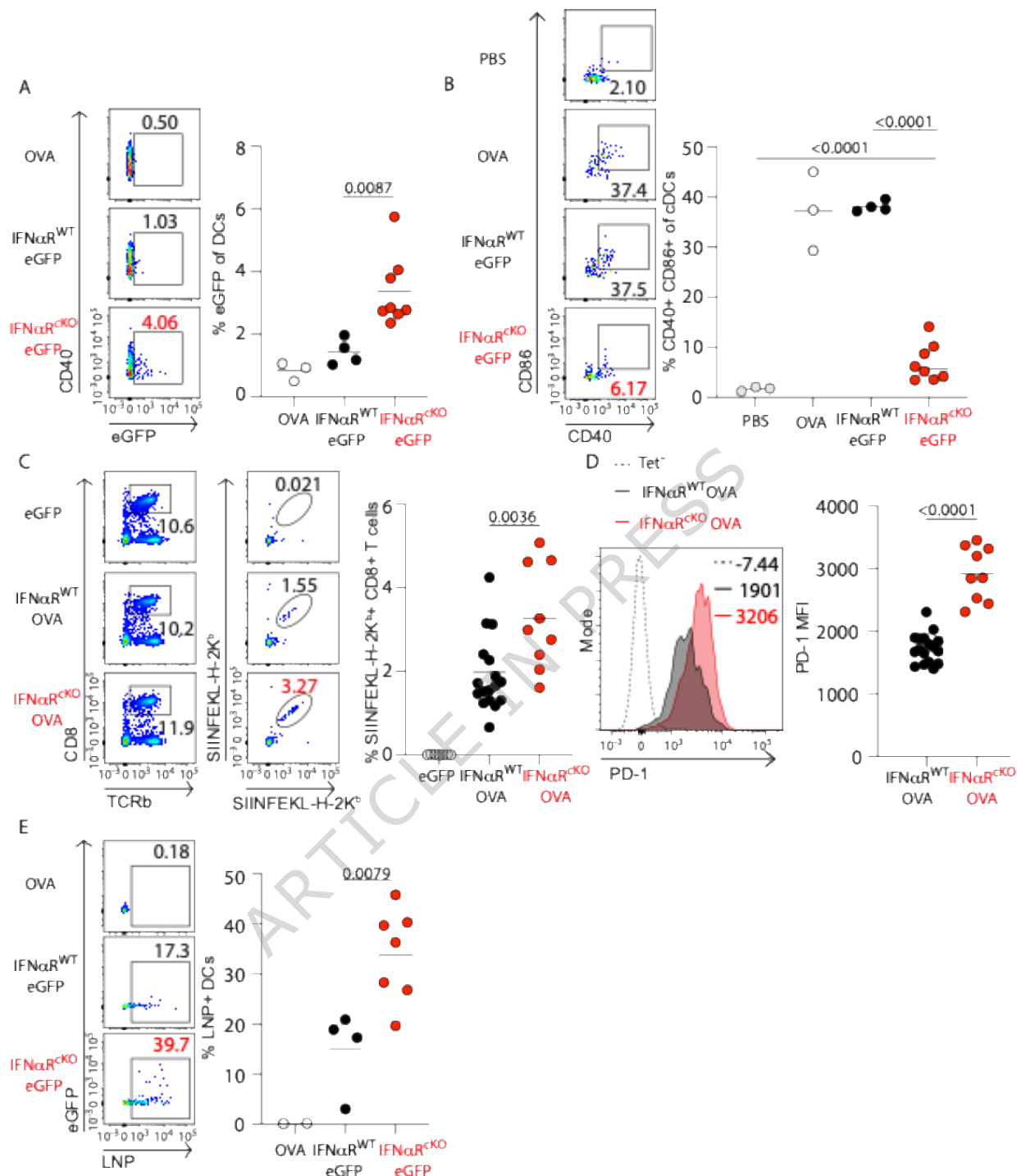


Figure 3. DC specific loss of IFN α R increases vaccine-specific CD8⁺ T cell responses.

(A) (Left) Representative flow plot of splenic cD11c⁺MHCII⁺ DCs expressing eGFP from IFN α R^{WT} or IFN α R^{cKO} mice. (Right) Percentage of eGFP expression in splenic DCs 24hr post mRNA-LNP immunization (5ug eGFP mRNA-LNP or 2.5ug OVA mRNA-LNP IV) in IFN α R^{WT} mice (black, n=4), or IFN α R^{cKO} mice (red, n=8). **(B)** (Left) Representative flow plot showing CD40⁺CD86⁺ splenic DCs after immunization with mRNA-LNP. (Right) Percentage of CD40⁺CD86⁺ splenic DCs from mice in Fig. 3A. **(C)** (Left) Representative flow plots of SIINFEKL-H2-K^b (OVA) specific CD8⁺ T cells. (Right) Percentage of OVA specific CD8⁺ T cells from IFN α R^{WT} mice (black, n=17) and IFN α R^{cKO} mice (red, n=9). 2.5ug of mRNA-LNP was administered IV. **(D)** (Left) Representative flow plot showing PD-1 expression of OVA specific TCR β ⁺CD8 α ⁺ T cells. (Right) PD-1 expression of TCR β ⁺CD8 α ⁺ T cells from mice in Fig. 3C. **(E)** (Left) Representative flow plot of splenic cD11c⁺MHCII⁺ DCs expressing fluorescent LNP from IFN α R^{WT} or IFN α R^{cKO} mice. (Right) Percentage of fluorescent LNP expression in splenic DCs 24hr post mRNA-LNP immunization (5ug DiD incorporated LNP eGFP mRNA-LNP or 2.5ug OVA mRNA-LNP IV) in IFN α R^{WT} mice (black, n=4), or IFN α R^{cKO} mice (red, n=7). All bars in (A)-(E) indicate mean. Data from (A), (B), (D), and (E) were compared using an unpaired two tailed students T test. Data from (C) was compared by a Mann Whitney test.

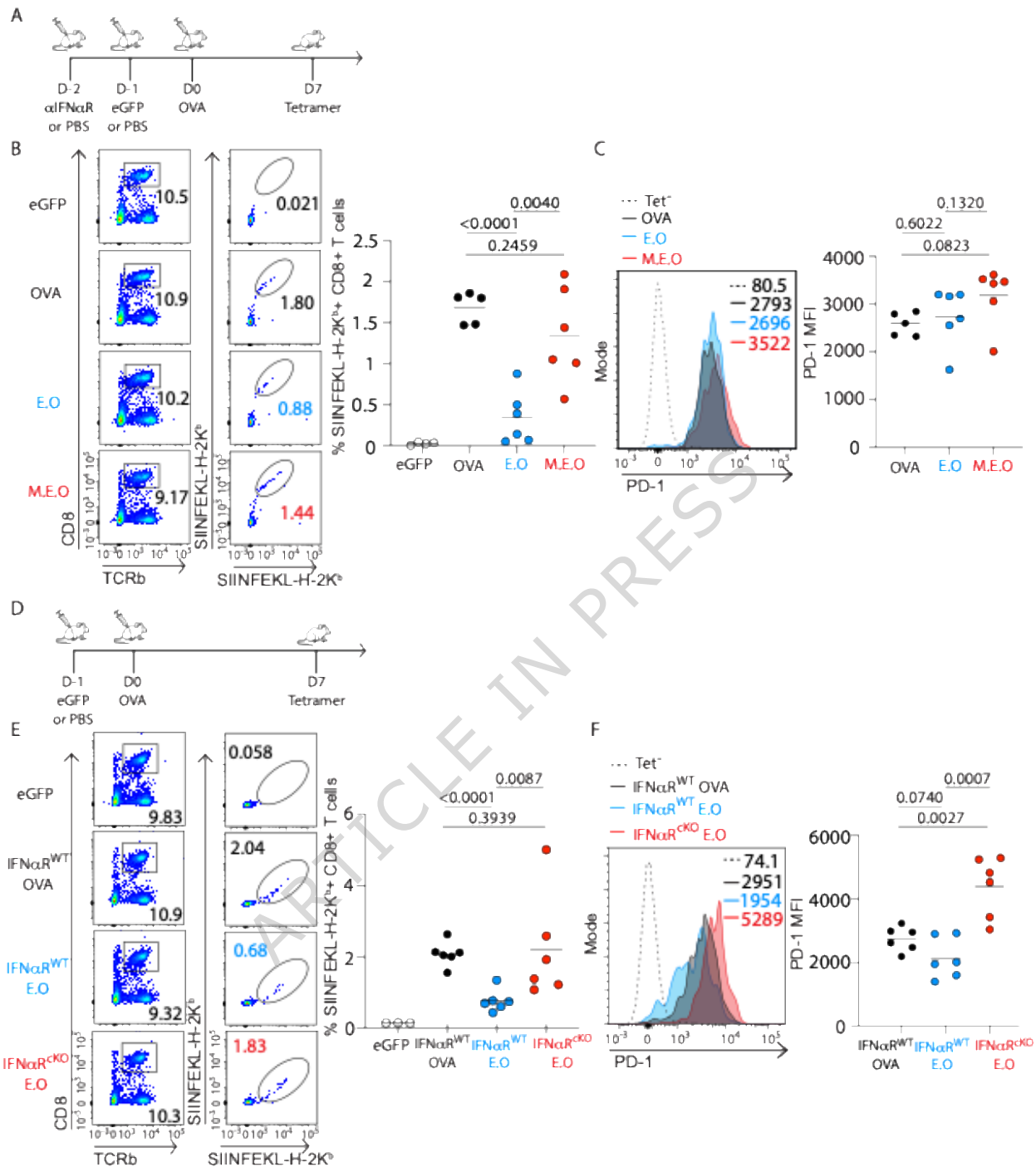


Figure 4. Inducing IFN before mRNA-LNP vaccination reduces vaccine efficacy.

(A) Experimental timeline for (B) and (C). Mice were injected IP with MAR1-5A3 antibody or PBS on Day -2. On Day -1 mice were immunized eGFP mRNA-LNP or PBS. The following day mice were immunized with OVA mRNA-LNP. Seven

days later mouse spleens were analyzed for SIINFEKL-H2-K^b specific CD8⁺ T cells. **(B)** (Left) Representative flow plots of SIINFEKL-H2-K^b (OVA) specific CD8⁺ T cells. (Right) Percentage of OVA specific CD8⁺ T cells from C57BL/6J wildtype mice (WT) given only OVA mRNA-LNP (black, n=5), eGFP mRNA-LNP then 24hr later given OVA mRNA-LNP (E.O) (blue, n=6), or MAR1-5A3 then 24hr later given eGFP mRNA-LNP followed by OVA mRNA-LNP 24hr hours after eGFP (red, n=6) (M.E.O). 2.5ug of mRNA-LNP was administered IV and 250ug of MAR1-5A3 was administered IP. **(C)** (Left) Representative flow plot showing PD-1 expression of OVA specific TCR β ⁺CD8 α ⁺ T cells. (Right) PD-1 expression of TCR β ⁺CD8 α ⁺ T cells from mice in Fig. 4B. **(D)** Experimental timeline for (E) and (F). Mice were injected with eGFP mRNA-LNP or PBS on Day -1. The following day mice were immunized with OVA mRNA-LNP. Seven days later mouse spleens were analyzed for SIINFEKL-H2-K^b specific CD8⁺ T cells. **(E)** (Left) Representative flow plots of OVA specific CD8⁺ T cells. (Right) Percentage of OVA specific CD8⁺ T cells from IFN α R^{WT} mice given just OVA mRNA-LNP (black, n=6), IFN α R^{WT} mice given eGFP mRNA-LNP then 24hr later given OVA mRNA-LNP (blue, n=6), and IFN α R^{CKO} mice given eGFP mRNA-LNP then 24hr later given OVA mRNA-LNP (red, n=6). **(F)** (Left) Representative flow plot showing PD-1 expression of OVA specific TCR β ⁺CD8 α ⁺ T cells. (Right) PD-1 expression of TCR β ⁺CD8 α ⁺ T cells from mice in Fig. 4E. All bars in (B), (C), (E), and (F) indicate mean. Data from (B) and (E) were compared using an unpaired two tailed students T test. Data in (C) and (F) were compared with either an unpaired two tailed students T test or a Mann Whitney test.

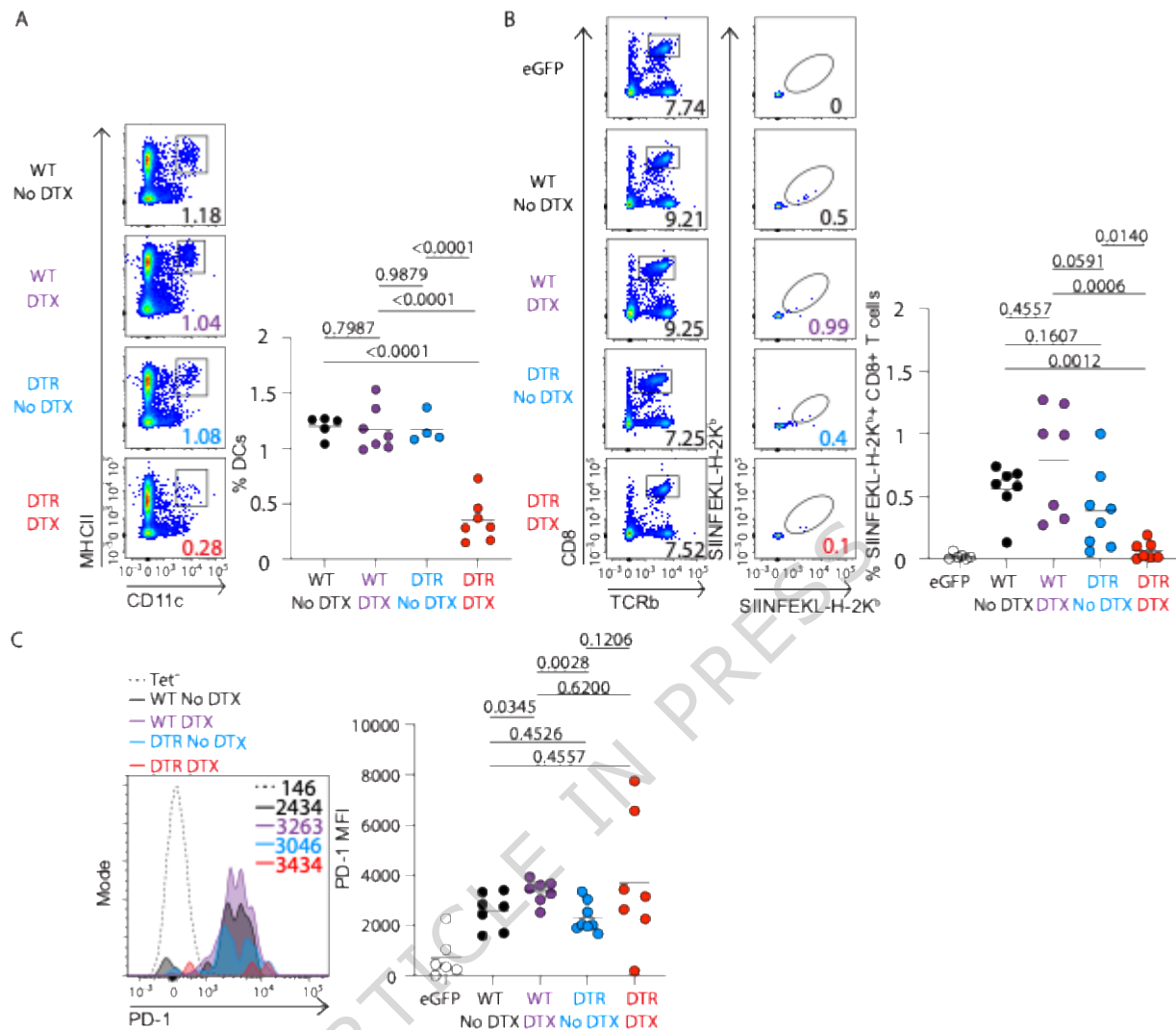


Figure 5. DCs are required to produce a CD8⁺ T cell response to mRNA vaccines.

(A) (Left) Representative flow plots of splenic MHCII⁺cD11c⁺ cells. (Right) Percentage of splenic MHCII⁺cD11c⁺ cells in C57BL/6J wildtype mice (WT) not given diphtheria toxin (black, n=5), WT mice given diphtheria toxin (purple, n=7), cD11c DTR mice not given diphtheria toxin (blue, n=4), and cD11c DTR mice given diphtheria toxin (red, n=7). **(B)** (Left) Representative flow plots of SIINFEKL-H2-K^b (OVA) specific CD8⁺ T cells. (Right) Percentage of OVA specific CD8⁺ T cells from WT mice not given diphtheria toxin mice (black, n=7), WT mice given diphtheria toxin (purple, n=7), cD11c

DTR mice not given diphtheria toxin (blue, n=8), and cD11c DTR mice given diphtheria toxin (red, n=7). Diphtheria toxin was administered on days -1, 1, 3, and 5 of mRNA-LNP administration at 4ng per gram of mouse. Mice were immunized with 2.5ug of either eGFP or OVA mRNA-LNP and CD8⁺ T cell were measured 7 days later. **(C)** (Left) Representative flow plot showing PD-1 expression of OVA specific TCR β ⁺CD8 α ⁺ T cells. (Right) PD-1 expression of TCR β ⁺CD8 α ⁺ T cells from mice in Fig. 5B. All bars in (A)-(C) indicate mean. Data was compared in (A) with an unpaired two tailed students T test. Data from (B) and (C) were compared with either an unpaired two tailed students T test or a Mann Whitney test.

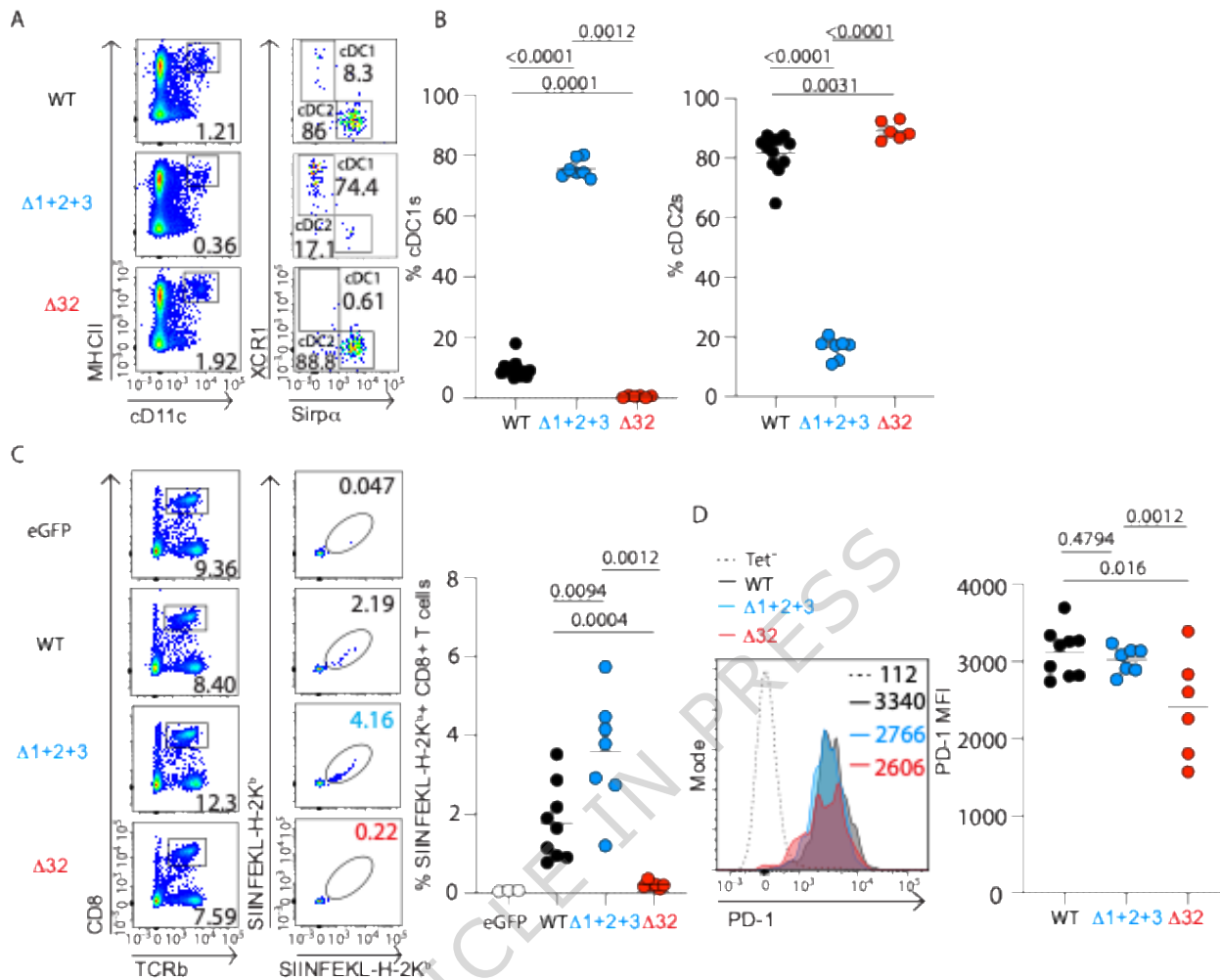


Figure 6. cDC1s are the major DC subset priming the CD8⁺ T cell mRNA-LNP vaccine immune response.

(A) Representative flow plots of the cDC1 population indicated by XCR1⁺Sirpa⁻ and the cDC2 population indicated by XCR1⁻Sirpa⁺ in C57BL/6J wildtype (WT) mice (black), $\Delta 1+2+3$ mice (blue), and $\Delta 32$ mice (red). **(B)** (Left) Data showing the percentage of cDC1 cells in WT, $\Delta 1+2+3$, or $\Delta 32$ mice. (Right) Data showing the percentage of cDC2 cells in WT, $\Delta 1+2+3$, or $\Delta 32$ mice. All cells are quantified by gating strategies used in Fig. 6A. **(C)** (Left) Representative flow plot of SIINFEKL-H2-K b (OVA) specific CD8⁺ T cells. (Right) Percentage of OVA specific CD8⁺ T cells from WT mice immunized with

OVA mRNA-LNP (black, n=9), $\Delta 1+2+3$ mice immunized with OVA mRNA-LNP (blue, n=7), and $\Delta 32$ mice immunized with OVA mRNA-LNP (red, n=6) measured 7 days post vaccination. All mice were immunized with 2.5ug of mRNA-LNP IV. **(D)** (Left) Representative flow plot showing PD-1 expression of OVA specific TCR β^+ CD8 α^+ T cells. (Right) PD-1 expression of TCR β^+ CD8 α^+ T cells from mice in Fig. 6C. All bars in (B)-(D) indicate mean. Data from (B)-(D) were compared using either an unpaired two tailed students T test or a Mann Whitney test.

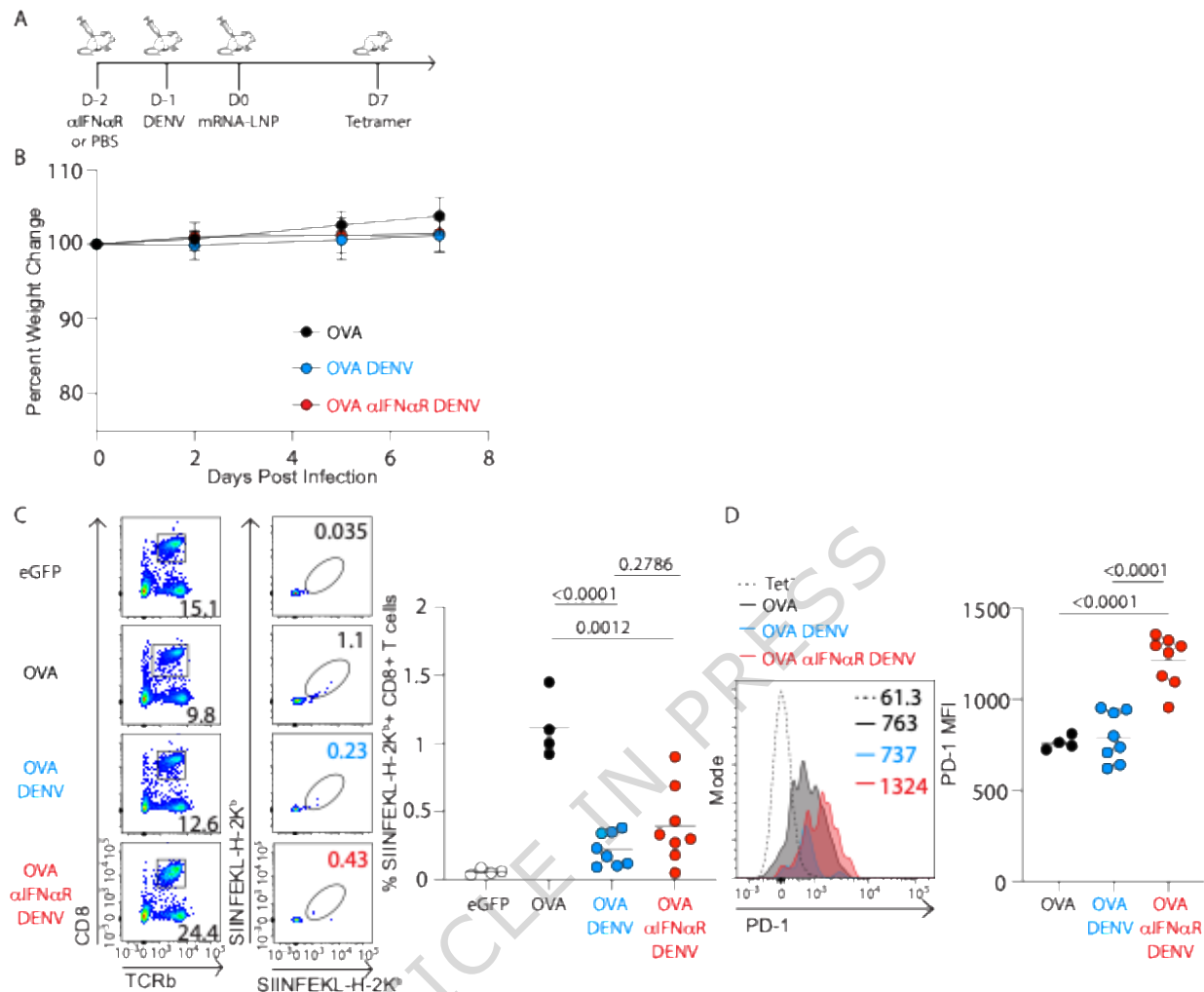


Figure 7. Vaccination during infection reduces CD8⁺ T cell response and cannot be rescued by IFNαR blockade.

(A) Experimental timeline for infectious challenge. Mice were injected IP with MAR1-5A3 antibody (α IFN α R) or PBS on Day -2. On Day -1 mice were inoculated with D220 virus. The following day mice were immunized with control eGFP mRNA-LNP or OVA mRNA-LNP. Seven days later mouse spleens were analyzed for SIINFEKL-H2-K^b specific CD8⁺ T cells. **(B)** Percent weight change of C57BL/6J wildtype mice (WT) either only given mRNA-LNP (black), mRNA-LNP after being infected with Dengue virus (blue), or given MAR1-5A3 24 hours before infection with Dengue virus then immunized

with mRNA-LNP a day later (red). **(C)** (Left) Representative flow plot of SIINFEKL-H2-K^b (OVA) specific CD8⁺ T cells. (Right) Percentage of OVA specific CD8⁺ T cells from WT mice given OVA mRNA-LNP only (black, n=4), Dengue infected mice given OVA mRNA-LNP (blue, n=8), or mice given MAR1-5A3 24 hours prior to infection with Dengue virus then immunized with OVA mRNA-LNP a day later (red, n=8). **(D)** (Left) Representative flow plot showing PD-1 expression of OVA specific TCR β ⁺CD8 α ⁺ T cells. (Right) PD-1 expression of TCR β ⁺CD8 α ⁺ T cells from mice in Fig. 7C. MAR1-5A3 was administered at 250ug IP, mRNA-LNP was administered at 2.5ug IV, and mice were infected with Dengue virus with 6.5×10^6 FFU IM. Error bars in (B) indicate \pm SD. All bars in (C)-(D) indicate mean. Data in (C) was compared using either an unpaired two tailed students T test or a Mann Whitney test. Data in (D) was compared using an unpaired two tailed students T test.

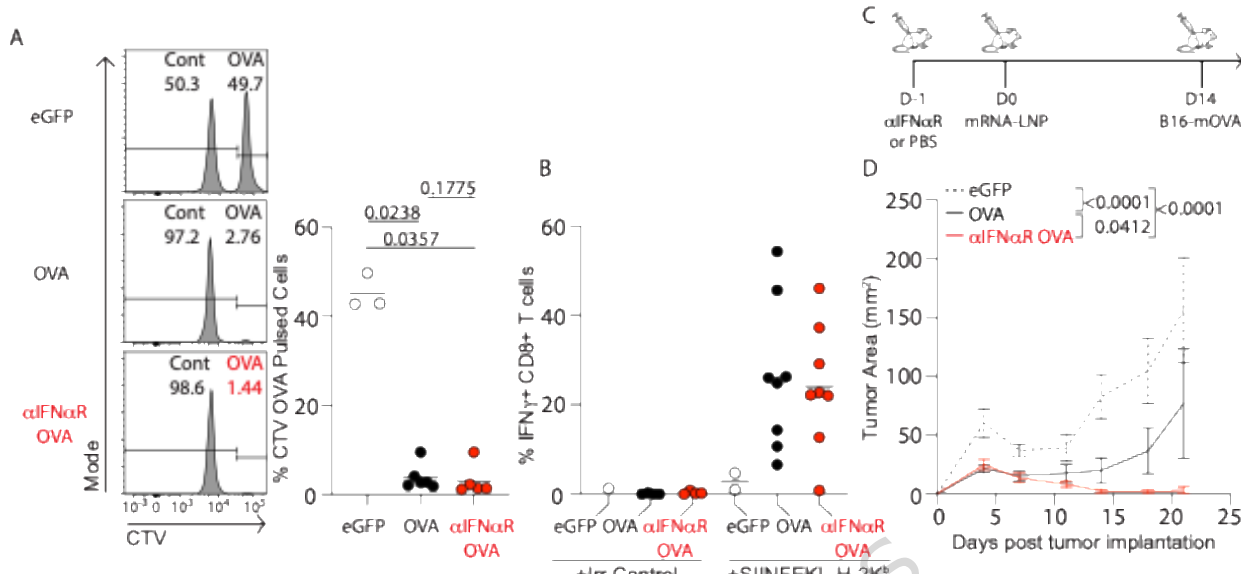


Figure 8. Vaccine-specific CD8⁺ T cells produced in the setting of IFN α R blockade are functional.

(A) (Left) Representative flow plot showing CTV low (100nM) labeled cells pulsed with an irrelevant peptide (IAPYYEAL; 1uM) and CTV high (1uM) labeled cells pulsed with OVA peptide (SIINFEKL; 1uM) that were administered 10 days post mRNA-LNP immunization. One million of each CTV labeled cell population was injected IV. C57BL/6J wildtype mice (WT) were given MAR1-5A3 (α IFN α R, red) or not (black) 24 hours before immunization with eGFP or OVA mRNA-LNP. MAR1-5A3 was administered at 250ug IP and mRNA-LNP was administered at 2.5ug IV. (Right) Percentage of the CTV high labeled population pulsed with OVA in WT mice given MAR1-5A3 (red, n=5) or not (black, n=6). **(B)** Percentage of IFN γ producing vaccine specific CD8⁺ T cells from mice immunized with 2.5ug of eGFP mRNA-LNP (white, n=1 and 2), OVA mRNA-LNP with MAR1-5A3 24hr prior to mRNA-LNP (red n=4 and 8), or not (black, n=4 and 8). Spleens were isolated 7 days post immunization and cells were stimulated with SIINFEKL-H2-K b peptide (10uM) for 5hr (right), or irrelevant peptide as

control (left). **(C)** Experimental timeline for tumor vaccination in (D). Mice were injected IP with MAR1-5A3 antibody or PBS on Day -1. The following day mice were immunized with control eGFP mRNA-LNP or OVA mRNA-LNP. Fourteen days later mice were implanted with B16-mOVA and followed for tumor growth. **(D)** Tumor growth curves of B16-mOVA C57BL/6J WT mice given MAR1-5A3 (red line, n=8) or not (black line, n=7) 24 hours before immunization with OVA mRNA-LNP. Control mice were administered eGFP mRNA-LNP (dotted line, n=5). Tumor measurements in (D) are pooled. All bars in (A) and (B) indicate mean. Data in (A) was compared using a Mann Whitney test. Error bars in (D) indicate S.E.M. Data in (D) was compared using a Two-way ANOVA followed by a Tukey's multiple comparisons test.